

# Measurement of the Plasma Beta in the Enormous Toroidal Plasma Device (ETPD)

K.L. DeRose \*,<sup>1,2</sup> C. Cooper,<sup>1</sup> P. Pribyl,<sup>1</sup> and W. Gekelman<sup>1</sup>

<sup>1</sup>*Department of Physics and Astronomy,*

*University of California, Los Angeles, CA 90095-1547*

<sup>2</sup>*Physics Department, Harvard University, Cambridge, MA 02138*

## Abstract

Utilizing the Enormous Toroidal Plasma Device (ETPD), a large toroidal chamber (30 m in circumference) with a Lanthanum Hexaboride (LaB<sub>6</sub>) cathode, a pulsed plasma was created the plasma beta ( $\beta = \frac{n_e k(T_e + T_i)}{B^2 / (2\mu_0)}$ ) was measured for various plasma parameters. Langmuir probe measurements give electron temperatures ranging from 5 to 30 eV as well as the ion saturation current as a function of distance into the plasma. Using a microwave interferometer to scale the Langmuir measurements, average electron densities were measured between  $2 \times 10^{11} \text{ cm}^{-3}$  to  $3 \times 10^{12} \text{ cm}^{-3}$ . Line widths of both the Helium neutral 4471 Å line and the Helium ion 4685 Å line were measured using a monochromator, giving an ion temperature of approximately 13 eV. Using fast photography, the plasma was found to have a more bifurcated structure than expected; an observation that is also confirmed via fast photography of strictly the 468 nm Helium II line. The ranges of values found for electron temperature, ion temperature, and density give a range of  $0.014 \leq \beta \leq 1.01$ .

PACS numbers:

---

\* Electronic Address: kderose@fas.harvard.edu

## I. INTRODUCTION

The plasma beta is an important dimensionless, scalable parameter in plasma physics. Astrophysical plasmas have features that span light years, making them impossible to recreate in the lab, but scaled experiments can be done. By defining beta as the particle kinetic energy density over the magnetic field energy density, it is possible to compare this dimensionless parameter between astrophysical plasmas and laboratory plasmas. Beta is explicitly defined in Equation 1, where  $n_e$  is the electron density,  $k$  is Boltzmann's constant,  $T_e$  is the electron temperature,  $T_i$  is the ion temperature,  $B$  is the magnetic field strength, and  $\mu_0$  is the vacuum permeability (Bellan 2006).

$$\beta = \frac{n_e k (T_e + T_i)}{B^2 / (2\mu_0)} \quad (1)$$

Generally, laboratory plasma has a low beta; for example, the LAPD plasma has  $\beta \sim 0.001$  (Gekelman et al. 1991), and even tokamaks have a hard limit of  $\beta = 0.08$  before the plasma becomes unstable (Wesson 2004). Astrophysical plasmas including the solar wind and the interstellar medium can have  $\beta \sim 1$  which is why it is important to be able to experimentally create high beta plasmas in order to study them.

In this experiment, a 30 m toroidal chamber was used to create a helical Helium plasma up to 120 m in length in an attempt to create a high beta laboratory plasma. This paper discusses the machine details, plasma profile, microwave interferometry density measurements, langmuir electron temperature measurements, and monochromator ion temperature measurements. Some preliminary conclusions about the plasma beta range reachable so far by the ETPD are then discussed.

## II. THE ENORMOUS TOROIDAL PLASMA DEVICE (ETPD)

The ETPD is composed of 16 vacuum chamber sections made from 1 in thick steel. These sections have inner dimensions  $2 \times 3$  m and are assembled into a torus of radius 5 m. This gives an inner chamber with a volume of  $\sim 188$  m<sup>3</sup>. A toroidal magnetic field is generated by 320, 0.75 in  $\times$  13 ft  $\times$  16 ft aluminum plates (with a rectangular hole in the middle that accomodates the chamber with 1-2 ft of clearance) that are grouped evenly in 10 plate groups around the central chamber. A vertical magnetic field is applied using concentric

coils near the top and bottom of the machine. The toroidal field strength is between 67 and 267 G, while the vertical field strength is between 1 and 10 G. The vertical magnetic field is necessary to give the plasma a helical path, in order to generate plasmas up to 120 m long. The machine is constructed from approximately 100 tons of steel (chamber) and 200 tons of aluminum (magnetic coils). A picture of the device is shown in Figure 1.

A 3.15 F capacitor bank (rated at 450 V) is used with a set of six switching transistors in order to create a 1 Hz pulsed plasma (with pulse lengths ranging from 15-120 ms). Four turbo pumps are used to keep the chamber at pressures between 0.5 mT and 5 mT. The system base pressure is  $5 \times 10^{-6}$  T. Ultra-high purity (UHP) helium is introduced into the chamber using a Mass Flow Controller (MFC) with rates between 12 and 26 sccm.

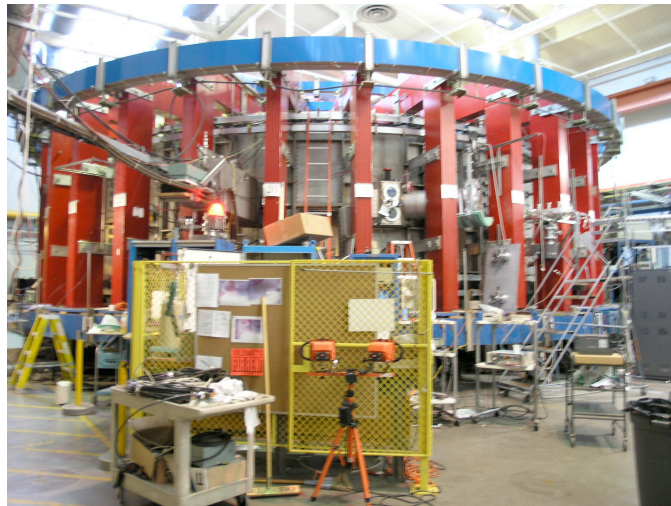


FIG. 1: Picture of the ETPD. The red plates help generate the toroidal field while the blue plates generate the vertical field. Windows along the side of the machine provide easy access for diagnostic probes and other experiments.

### III. THE SOURCE

The cathode is composed of 4,  $4 \times 4$  in tiles of Lanthanum Hexaboride ( $\text{LaB}_6$ ).  $\text{LaB}_6$  is a refractory ceramic that is stable in vacuum and has a melting point of  $2210^\circ \text{C}$ . It has a very low work function and one of the highest electron emissivities known (Ahmed and Broers 1972). Unlike plasma cathodes that rely on coatings that are extremely sensitive to air exposure,  $\text{LaB}_6$  can be brought up to air without requiring a lengthy recoating process.

The tiles are held in place by a molybdenum mesh near a 5/8 inch thick graphite heater. A larger molybdenum mesh mounted about 13 inches away from the cathode serves as the anode and the discharge voltage is applied between them. Thus, as the heater heats up the  $\text{LaB}_6$ , electrons stream from the negative cathode to the positive anode, ionizing a fraction of the neutral helium atoms in the chamber. These ions, electrons, and neutrals then travel further past the anode forming the visible plasma spiral. Figures 2 and 3 show the rings of a helium plasma taken with a 468 nm ion line filter and at all frequencies.

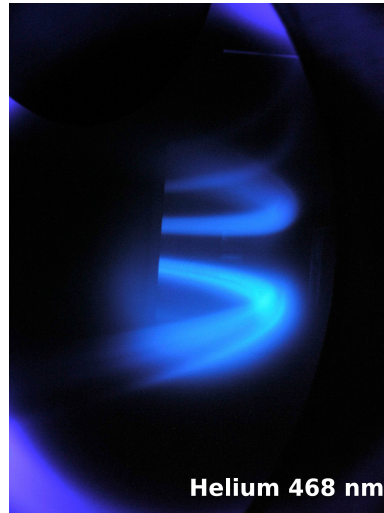


FIG. 2: Helium 656 nm ion line picture of pulsed plasma rings.

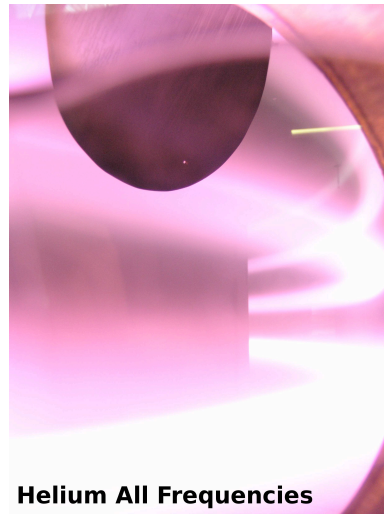


FIG. 3: Helium all frequencies picture of pulsed plasma rings.

#### IV. LANGMUIR PROBE MEASUREMENTS

A two-sided disk Langmuir probe made of tantalum was used to make IV curve measurements as well as ion saturation current measurements in Section V. The disk has a radius of 0.16 cm, making the probe surface area approximately  $0.16 \text{ cm}^2$  (taking into account both sides). It is important to note that when the probe was taken out of the machine, it was coated in what appeared to be graphite dust, which may have severely altered the collecting area of the probe, making the subsequent calculations imprecise.

IV curves were measured using a fast voltage sweeper, and from the IV curves and their subsequent electron distributions, the electron temperatures were determined. Figure 4 shows two example IV curves with their calculated distribution functions. From the figure, it is clear that the first case (subfigures a and b) has a great deal more fast electrons than expected, while the second case has a more normal, single temperature distribution (subfigures c and d). The measurements in general seem divided evenly between these two cases. The latter prove easier to analyze by more conventional methods, while the former cannot easily be explained by a single thermal distribution. Many IV curves were taken at various pressures, discharge voltages, pulse lengths, and heater temperatures, yielding electron temperatures of 5-30 eV through the same analysis.

#### V. ION SATURATION CURRENT PLASMA PROFILE

A significant amount of RF noise was present in both Langmuir and ion saturation measurements, making it necessary to electrostatically shield the power source. With the Langmuir probe as a load across the batteries, the effective voltage was  $V_{bias} \sim 130 \text{ V}$ . This is a reasonable value for measuring the ion saturation current, as most of the electrons have energies below 30 eV.

The ion saturation current is given in Equation 2 where  $A$  is the area of the probe head (the factor of 2 is included because it is a two-sided probe),  $n_e$  is the electron density,  $k$  is Boltzmann's constant,  $T_e$  is the electron temperature, and  $m_I$  is the ion mass (Chen 1984).

$$I_{SAT} = (2A)n_e c_s = (2A)n_e \sqrt{\frac{kT_e}{m_I}} \quad (2)$$

Because having a probe in contact with a magnetized plasma fundamentally alters the

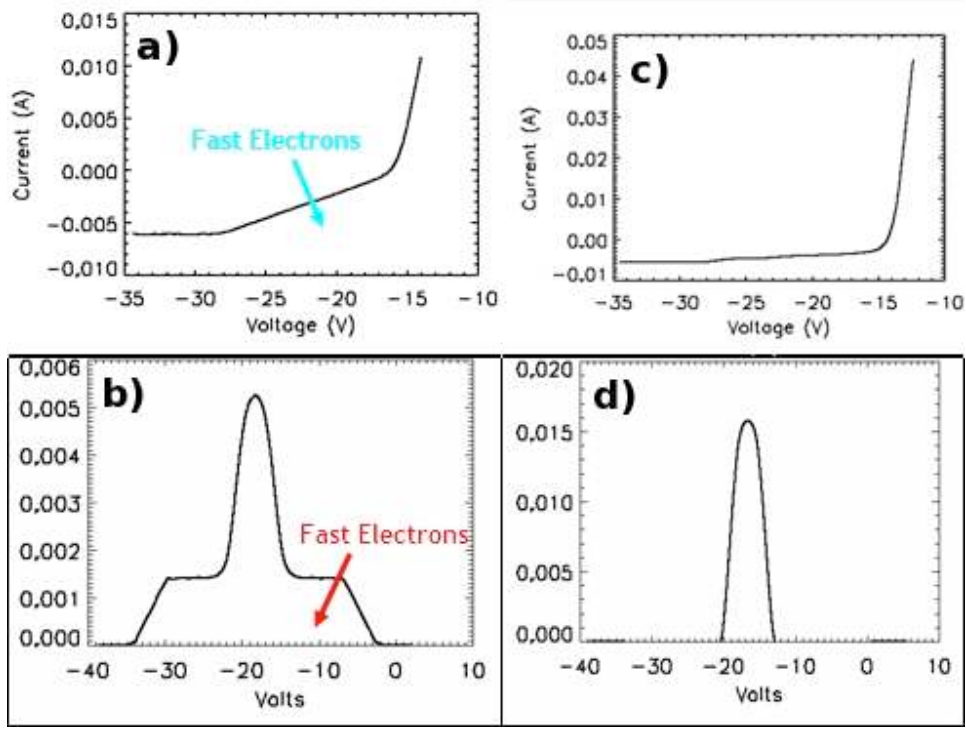


FIG. 4: a) IV Curve for  $T_e=7.15$  eV. Note that there is a significant bump of from fast electrons. b) Distribution function for a). The fast electrons give the appearance of a two temperature plasma and cannot easily be analyzed in conventional ways. c) IV Curve for  $T_e=6.58$  eV. This represents one of the more normal Langmuir curves, because the fast electron tail is small. d) Distribution function for c). Only one temperature of electrons appears to be present.

measurement, the density calculated from the ion saturation current measurements is not as reliable as the microwave interferometer measurements discussed in Section VI. Since it was also not clear what the effective area of the probe was due to deposits on the probe head, this makes calculations using Equation 2 even more imprecise. However, the relative densities are accurate and can help give us an idea regarding the density profile of the plasma. Figure 5 is a plot of ion saturation current vs. distance into the plasma. The data in the figure was taken with a discharge voltage and current of 240 V and 175 A (42 kW), a pressure of 4 mT, and a toroidal magnetic field of 160 G.

The profile is much more peaked than expected, which could potentially mean the probe was not traveling through the exact center of the discharge. The full width at half max (FWHM) is approximately 15 cm, which will be the diameter of the plasma used in the calculations in Section VI.

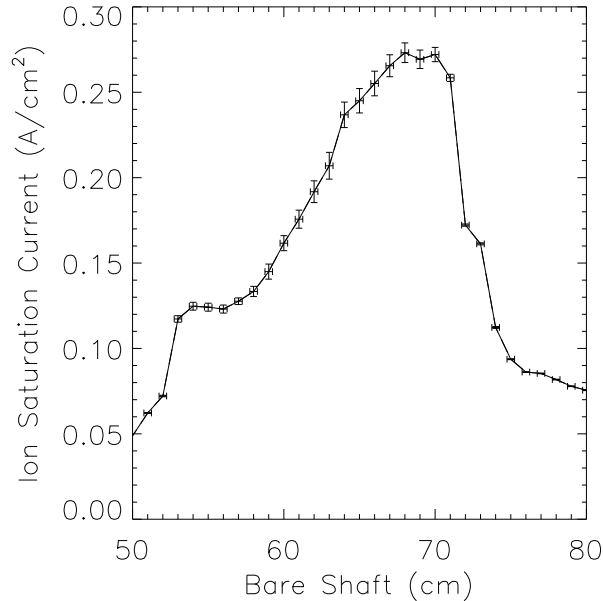


FIG. 5: Ion saturation current ( $\text{A}/\text{cm}^2$ ) vs. distance into plasma (cm). Vertical error bars represent the standard deviation over the pulse peak and horizontal error bars represent the measurement error.

## VI. MICROWAVE INTERFEROMETER DENSITY MEASUREMENTS

A microwave interferometer was used to take line-averaged density measurements of the plasma during the turn-off of the plasma light curve. A schematic of the experimental setup is shown in Figure 6. Two microwave sinusoidal signals with frequencies 96 and 96.1 GHz are generated and one beam is sent through a plasma of diameter  $L$  and bounces back off the far wall of the machine. The signal travels a total distance of  $2L$  after passing through plasma and thus experiences a phase shift proportional to the amount of plasma it has passed through.

By counting the number of fringes seen in the turn-off of the plasma, it is possible to find the line-averaged density. In this particular setup, the quantity  $\langle n_e L \rangle$  is determined by Equation 3 where  $n_e$  is the electron density,  $L$  is the diameter of the plasma determined from Figure 5, and  $N_{fringes}$  is the number of fringes counted in the microwave interferometry trace.

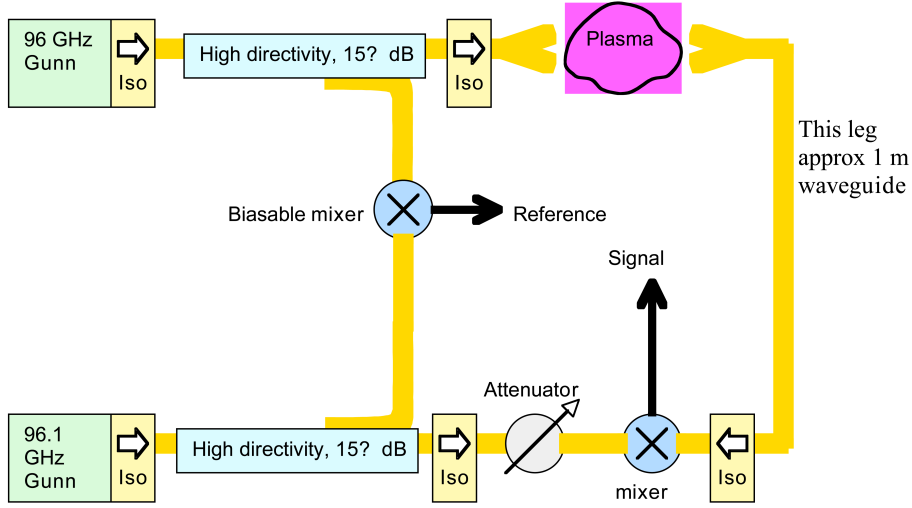


FIG. 6: A schematic of the experimental microwave interferometer setup.

$$\langle n_e L \rangle = 1.1385 \times 10^{13} N_{fringes} \quad (3)$$

The microwave interferometry trace associated with the data in Figure 5 is shown in Figure 7. In this figure, at least 28 fringes can be identified, giving a line-averaged electron density of  $1.89 \times 10^{13} \text{e}^-/\text{cm}^3$ .

## VII. MONOCHROMATOR ION TEMPERATURE MEASUREMENT

Because the  $\beta$  parameter is dependent on the electron temperature and the ion temperature, it is important to first determine if the ion temperature is significant in comparison with the electron temperature and second find a reliable way to measure it. Because the shape of the ion spectral line is determined by the doppler effect, the width of a spectral line is directly related to the temperature of the emitting atoms. Other line broadening mechanisms such as Zeeman splitting and the Stark effect were negligible. Equation 4 gives the expected thermal broadening for a spectral line where  $\Delta\lambda_D$  is the FWHM of the line,  $\lambda$  is the true wavelength of the line,  $T_i$  is the ion temperature, and  $\mu$  is the ion mass.

$$\Delta\lambda_D = 7.7 \times 10^{-5} \lambda \sqrt{\frac{T_i}{\mu}} \quad (4)$$

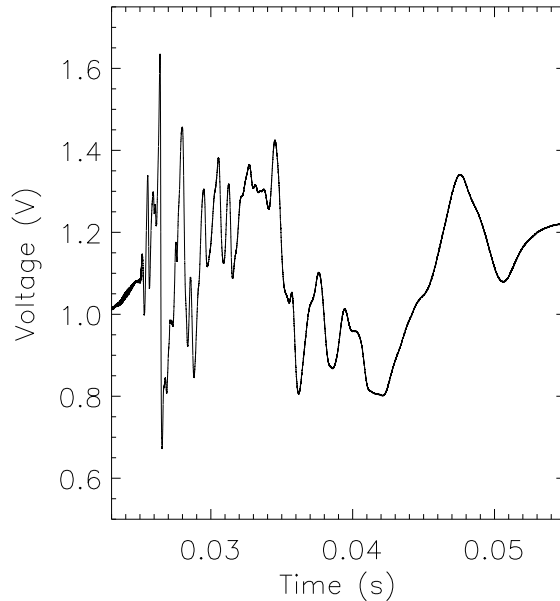


FIG. 7: Microwave interferometer fringes for use in scaling the ion saturation measurements discussed in Section V. At least 28 fringes are identified.

A large lens was used to focus light from the first ring of plasma ( $\sim 90^\circ$  from the source) onto a fiber bundle shaped into a vertical slit in order to maximize the amount of light collected. A 1 m monochromator with a R928 Hamamatsu Photomultiplier tube was then connected to an amplifier (gain 100) and the slit widths were varied in order to optimize the collected light and instrumental resolution.

The goal was to measure the FWHM of the  $4685 \text{ \AA}$  ion line, and while a 1 m monochromator should technically have sub-angstrom resolution, this proved difficult to achieve due to the faintness of the line. The signal measured ( $S(\lambda)$ ) is a convolution between the actual ion line ( $L(\lambda)$ ) and the instrumental response function ( $I(\lambda)$ ) as described in Equation 5. Therefore, the ion line can be deconvolved from the instrumental response function using Equation 6.

$$S(\lambda) = I(\lambda) \otimes L(\lambda) \quad (5)$$

$$L = IFT\left(\frac{FT(S)}{FT(I)}\right) \quad (6)$$

In discharge plasmas, the neutral temperature is generally much less than the ion tem-

perature. It was assumed the neutrals were cold and the 4471 Å neutral line was used to determine the instrumental response function (the line width at essentially 0 temperature). The deconvolution was calculated using the Spectral Line Deconvolution Program written by G. Petrov, and the results are displayed in Figure 8 (Petrov 2004).

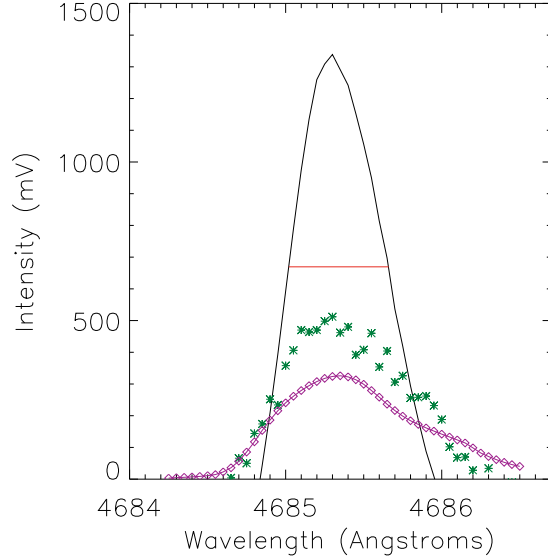


FIG. 8: The deconvolution of the 4685 Å ion line (PMT Voltage (mV) vs. Wavelength (Å)). A statistical error of 15% and the dark current is taken into account in the deconvolution. The purple diamonds represent the instrumental response from the 4471 Å neutral line, the green asterisks represent the measured 4685 Å ion line, the black curve is the deconvolution, and the red line indicates the FWHM of the deconvolution. From this the FWHM of the ion line is determined to be  $\sim 0.65$  Å.

From the deconvolution, the FWHM of the ion line is  $\sim 0.65$  Å, which gives us an ion temperature of  $\sim 13$  eV. This is a very high number considering that under these conditions, the electron temperature was closer to 5 eV, although there were fast electrons in the tail of the distribution function ( $f_e(v)$ ). More work must be done to confirm the accuracy of this measurement, however, it seems that the ions are quite energetic, a fact that makes sense given the ion/electron equilibration time is around 15 ms (the plasma is pulsed for at least 30 ms and up to 120 ms).

## VIII. BETA CALCULATIONS

In the previous sections, the experimentally determined ranges for electron density, electron temperature, and ion temperature have been discussed. Using Equation 1, it is then possible to find the range for beta currently achievable with the ETPD. Using minimum parameters of  $T_e=5$  eV,  $T_i=1$  eV, and  $n_e=2\times 10^{12}e^-/\text{cm}^3$ , a minimum  $\beta=0.014$  was calculated. Using maximum parameters of  $T_e=30$  eV,  $T_i=13$  eV, and  $n_e=2\times 10^{13}e^-/\text{cm}^3$ , a maximum  $\beta=1.01$  was calculated. A  $\beta > 1$  plasma is the goal of this experiment, and this preliminary data shows that it is feasible.

## IX. ACKNOWLEDGMENTS

This work was supported by the National Science Foundation through the Research Experience for Undergraduates (REU) program. The work was done at UCLA under the auspices of the Basic Plasma Science Facility which is funded by the Department of Energy and the National Science Foundation.

## X. BIBLIOGRAPHY

Ahmed, H. and Broers, A.N., 'Lanthanum Hexaboride Electron Emitter', J. Appl. Phys. 43, 2185 (1972)

Bellan, Paul M., Fundamentals of Plasma Physics, (2006), Cambridge University Press, Cambridge.

Chen, F.F., Introduction to Plasma Physics and Controlled Fusion, (1984) 2nd ed., Plenum Press, New York.

Gekelman, W., Pfister, H., Lucky, Z., Bamber, J., Leneman, D., and Maggs, J, 'Design, construction, and properties of the large plasma research device - The LAPD at UCLA', Rev. Sci. Instrum. 62, 2875 (1991)

Petrov, G.M., 'A simple algorithm for spectral line deconvolution', JQSRT 72, 281-287 (2002)

Wesson, J., Tokamaks, (2004), Clarendon Press, Oxford